

## 알칼리 전지의 정극재료로서 쓰이는 수산화 니켈에 대한 전기화학적 고찰

尹 英 基 · 邊 秀 一

韓國科學技術院 材料工學科

### The Electrochemical View of Nickel Hydroxide as Cathode Materials in Alkaline Battery

YOUNG-GI YOON and SU-IL PYUN

*Department of Materials Science and Engineering,  
Korea Advanced Institute of Science and Technology,  
# 373-1 Kusong-Dong, Yusong-Gu, Daejeon 305-701, Korea*

#### 1. Introduction

Chemically or electrochemically deposited nickel hydroxide conventionally used as cathode materials in the alkaline battery can be regarded as a dispersed hydrous oxide where oxygen is present not just as a bridging species between metal ions, but also as  $O^-$ ,  $OH^-$ , and  $OH^-$ , and  $OH_2$  species, i. e., incoordinated terminal group form.<sup>1)</sup> In many cases nickel hydroxide, when in contact with aqueous media, contain considerable quantities of loosely bound and trapped water, plus, occasionally, electrolyte species. The more open structure of nickel hydroxide leads to greater reactivity for various reactions, e.g., charge storage and electrochromic reactions, and electrocatalysis.

There has long been an interest in the behaviour of the nickel hydroxide electrode because of its use as the cathode in cadmium/nickel oxide and iron/nickel hydroxide batteries. More recently, there has been renewed interest because of the advent of hydrogen/nickel hydroxide batteries. In addition

to batteries, nickel hydroxide electrodes are also used in water electrolyzers,<sup>2)</sup> organic synthesis,<sup>3)</sup> electrochromic devices<sup>4, 5)</sup> and microelectrochemical transistor.<sup>6)</sup>

The battery storage reaction involves the oxidation of  $Ni(OH)_2$  during charge and the reduction of the oxidized product during discharge. The reactions apparently proceed via a topochemical pathway without the formation of soluble intermediates. This has complicated elucidation of the overall reaction and the charge/discharge mechanisms.

The present review article is aimed firstly, at overlooking the papers on the nickel hydroxide electrode previously published in the literature involving structural and textural characteristics, electrochemical processes, transport processes, self discharge, electrochromism, and additive effects from the electrochemical view points and secondly, at providing several basic ideas chiefly on the proton diffusion for the future work.

## 2. Structural and textural characteristics of the nickel hydroxide electrode

A major advance in the understanding of the reactions of the nickel oxide electrode was made by Bode and co-workers.<sup>7)</sup> They established the existence of two forms of  $\text{Ni}(\text{OH})_2$ , one is an anhydrous form with a brucite structure, called  $\beta$ - $\text{Ni}(\text{OH})_2$ , and the other is a hydrated form which they called  $\alpha$ - $\text{Ni}(\text{OH})_2$ . Oxidation of  $\beta$ - $\text{Ni}(\text{OH})_2$  produced  $\beta$ - $\text{NiOOH}$  and oxidation of  $\alpha$ - $\text{Ni}(\text{OH})_2$  produced  $\gamma$ - $\text{NiOOH}$ . Changes in the crystal forms of nickel hydroxide during charge and discharge together with the associated change in density, are shown in Fig. 1.<sup>8)</sup>

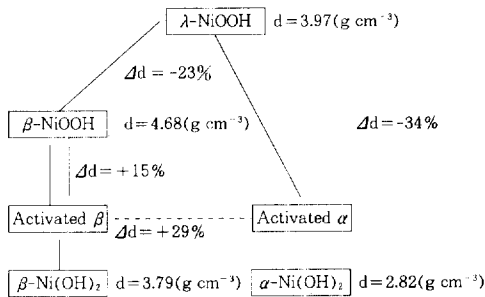


Fig. 1 Density and crystal change in nickel hydroxide active material on charge and discharge.<sup>8)</sup>

### 2.1 $\beta$ - $\text{Ni}(\text{OH})_2$

The X-ray and neutron diffraction results indicate that  $\beta$ - $\text{Ni}(\text{OH})_2$  has a brucite C6-type structure and is isomorphous with the divalent hydroxides of Ca, Mg, Fe, Co, and Cd. The structure is shown in Fig. 2.<sup>6)</sup> The crystal consists of stacked layers of nickel-oxygen octahedra. The nickels are all in the (0001) plane and are surrounded by six hydroxyl groups, which lie alternately above and below the (0001) plane. The fractional coordinates are, for nickel, 0,0,0, and, for oxygen, 1/3, 2/3, z and 2/3, 1/3, z. Values for the crystallographic parameters are given in Table 1.<sup>6)</sup> These are for well-crystallized  $\beta$ - $\text{Ni}(\text{OD})_2$ .

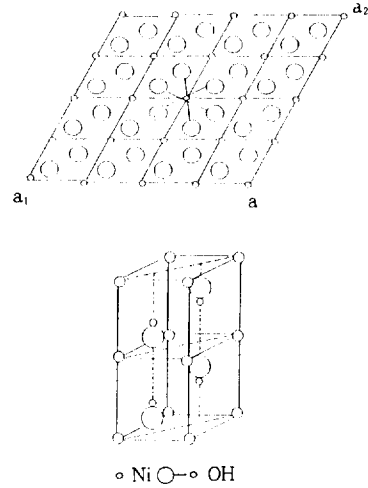


Fig. 2 The crystal structure of  $\beta$ - $\text{Ni}(\text{OH})_2$ : (a) the structure within the basal plane; (b) the stacking along the c-axis.<sup>6)</sup>

Table 1. Crystallographic parameters for  $\beta$ - $\text{Ni}(\text{OD})_2$ <sup>6)</sup>

Parameter	Value/nm
$a_0$	0.3126
$c_0$	0.4593
Ni-O bond length	0.2073
O-D bond length	0.0973
Ni-Ni bond length	0.3126

### 2.2 $\alpha$ - $\text{Ni}(\text{OH})_2$

Another form of  $\text{Ni}(\text{OH})_2$  with a highly hydrated structure is  $\alpha$ - $\text{Ni}(\text{OH})_2$ . The hydrated hydroxide has the formula  $\text{Ni}(\text{OH})_2 \cdot x\text{H}_2\text{O}$ , where x is between 0.5 and 0.7. Bode proposed a layered structure for  $\alpha$ - $\text{Ni}(\text{OH})_2$  similar to that for  $\beta$ - $\text{Ni}(\text{OH})_2$ .<sup>7)</sup> The proposed structure is essentially identical to that shown for  $\beta$ - $\text{Ni}(\text{OH})_2$  in Fig. 2 except that between the (0001) planes there are water molecules that are hydrogen bonded to the Ni-OH groups, resulting in an expansion of the c-axis spacing to about 0.8nm.

Subsequent X-ray and infrared spectroscopic study<sup>9)</sup> has shown that  $\alpha$ - $\text{Ni}(\text{OH})_2$  has a disordered turbostratic structure. The c-axis spacing is

constant, but the layers are randomly oriented as shown in Fig. 3.<sup>8)</sup> By electron microscopy<sup>10)</sup> turbostratic nickel hydroxide appears as aggregates of thin crumpled sheets, without any definite shape.

Turbostratic nickel hydroxide aged completely to crystallized  $\text{Ni}(\text{OH})_2$  within a few hours in alkali solution or pure aqueous medium at room temperature. Le Bihan and Figlarz<sup>10)</sup> have shown without any ambiguity that the mechanism of recrystallization proceeds via the solution by dissolution of the turbostratic phase and nucleation and growth of crystallized  $\beta$ (II)  $\text{Ni}(\text{OH})_2$  from the solution.

### 2.3 $\beta$ -NiOOH

$\beta$ -NiOOH has been identified as the primary oxidation product of electrodes containing  $\beta$ - $\text{Ni}(\text{OH})_2$ .<sup>7)</sup> It appears that  $\beta$ - $\text{Ni}(\text{OH})_2$  is oxidized to the trivalent state without major modifications to the brucite structure. The unit cell dimensions change from  $a_0=0.3126\text{nm}$  and  $c_0=0.4605\text{nm}$  for  $\beta$ - $\text{Ni}(\text{OH})_2$  to  $a_0=0.282\text{nm}$  and  $c_0=0.485\text{nm}$  for  $\beta$ -NiOOH.

The overall reaction for the electrochemical formation of  $\beta$ -NiOOH is usually given as



During the reaction protons are extracted from the brucite lattice. Infrared spectra<sup>11, 12)</sup> show that

during charge the sharp hydroxyl band at  $3644\text{cm}^{-1}$  disappears. This absorption is replaced by a diffuse band at  $3450\text{cm}^{-1}$ . The spectra indicate a hydrogen-bonded structure for  $\beta$ -NiOOH with no free hydroxyl groups.

### 2.4 $\gamma$ -NiOOH

$\gamma$ -NiOOH is the oxidation product of  $\alpha$ - $\text{Ni}(\text{OH})_2$ . It is also produced on overcharge of  $\beta$ - $\text{Ni}(\text{OH})_2$ , particularly when the charge is carried out at high rates in high concentration of alkali.<sup>7)</sup> The material has a layered structure with a spacing of  $0.72\text{nm}$  between layers.  $\gamma$ -NiOOH always contains small quantities of alkali metal ions and water in between the van der Waals gaps of the layers.

Electron microscopy showed that the oxidation is related to the breaking up of the turbostratic hydroxide sheets. This result can be interpreted by assuming that oxidation induces some strains in relation to the large difference of the nickel-nickel distance in the (001) planes in the oxidized NiOOH  $\gamma$ -phase and in the turbostratic hydroxide; these strains are relieved by sheet fragmentation.<sup>8)</sup>

Indeed,  $\gamma$ (III) has two different morphological characteristics, alpha-generated  $\gamma$ (III) in the form of broken crumpled sheets and beta-generated  $\gamma$ (III) in the form of small platelets. The strains induced by the very large difference in interlamellar spacing along the c axis between  $\gamma$ (III) and  $\beta$ (II) are more readily relaxed as the number of planes in the [001] direction is small, i.e. the platelet par-

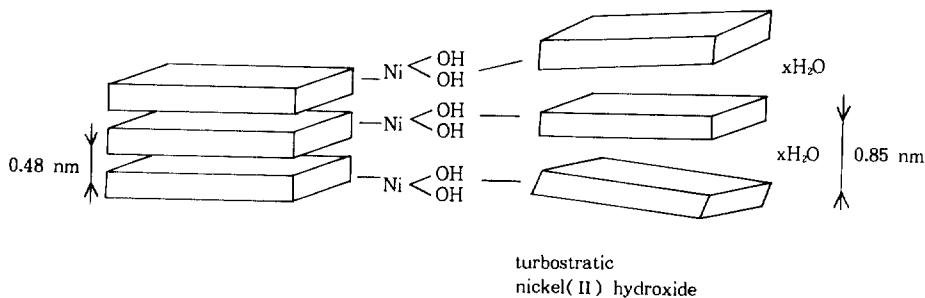


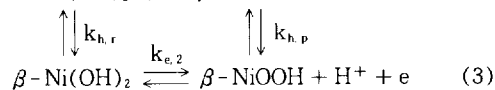
Fig. 3. Structural schemes of crystallized  $\beta$ (II)- and turbostratic  $\alpha$ - $\text{Ni}(\text{OH})_2$ .<sup>8)</sup>

ticles are thinner. For thicker particles, the  $\beta$ (II)  $\rightarrow$   $\beta$ (III) transformation is promoted in order to minimize the induced strains along [001].

### 3. Electrochemical and chemical processes related to the nickel hydroxide electrode

The battery storage reaction involves the oxidation of  $\text{Ni}(\text{OH})_2$  during charge and the reduction of the oxidized product during discharge. These reactions apparently proceed via a topochemical pathway without the formation of soluble intermediates.<sup>13,14</sup> This has complicated elucidation of the overall reaction and the charge/discharge mechanisms.<sup>13-15</sup>

The simplest representation of those electrochemical and chemical processes related to the nickel hydroxide electrode has been given in terms of a square reaction scheme such as:<sup>13</sup>

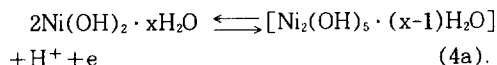


where the ks are the corresponding rate constants; e stands for the electrochemical reactions; h for the chemical reactions; r, for the reactants and p, for the products. The proposed reaction scheme, however, leaves open the possibility of a contribution from the crossed processes which remain unnoticed, at least with the perturbation technique then used.

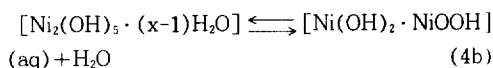
#### 3.1 Rate processes related to the hydrated nickel hydroxide

Provided that the overall anodic process under potentiodynamic conditions is expressed by the overall reaction (2) or (3), a possible reaction path which may account for the kinetic behavior should imply a series of single electron transfer and chemical steps as follows.<sup>15</sup> The initial stage is the proton release from the hydrated  $\text{Ni}(\text{OH})_2$

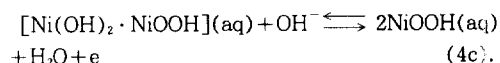
lattice on the positively charged nickel surface



The proton diffusion out of the electrochemical interface is assisted by the electrical field located there. Step (4a) involves a partially hydrated intermediate which undergoes a structural rearrangement through a chemical reaction



and finally

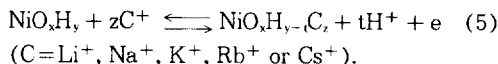


The formation of the  $\text{NiOOH}$ -species is equivalent either to the accumulation of  $\text{Ni}(\text{III})$  species or to the creation of 3-d holes in the film.<sup>16</sup> Whatever the case, the reaction path (4a)-(4c) implies an increasing deprotonation of the insoluble film, so that the Ni/O atomic ratio remains constant, the H/O ratio decreases, and the Ni/H ratio increases in passing from the hydrated  $\text{Ni}(\text{OH})_2$  to the  $\text{NiOOH}$  species. Several groups of workers<sup>15, 17</sup> have also proposed that intrinsically less active materials such as  $\text{Ni}_3\text{O}_3(\text{OH})_4$  or  $\text{Ni}_3\text{O}_4 \cdot x\text{H}_2\text{O}$  appear as intermediates in the reduction of  $\beta$ - $\text{NiOOH}$ . Whether these materials are true compounds, or phases in a solid solution system is unclear yet.

#### 3.2 Alkaline cation incorporation into nickel hydroxide

Alkaline cation incorporation during oxidation reactions has been proposed in other work,<sup>17-19</sup> assuming a simultaneous  $\text{OH}^-$  incorporation. From the electrochemical quartz crystal microbalance study, Faria et al.<sup>20</sup> suggested an exchange reaction in which the oxidation(reduction) process is accompanied by the deintercalation(intercala-

tion) of a relatively large number of "light" cations, simultaneously with the intercalation (deintercalation)\* of a small number of heaviest cations. The proposed exchange reaction is:



They reported that, in the anodic (cathodic) cycle, a large number of protons are deintercalated (intercalated) and a smaller number of cations are intercalated (deintercalated) in the oxide film. Also, as the highest molar fraction corresponds to cations with the lowest atomic weight, more Li<sup>+</sup> ions are exchanged than, for example, Cs<sup>+</sup> ions. In spite of the fact that a larger number of Li<sup>+</sup> ions are exchanged, the effect on the volume changes are the same as that of the biggest Cs<sup>+</sup> ions, that are exchanged in a smaller number.

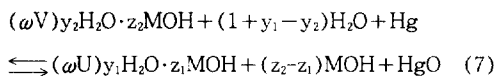
### 3.3 Reversible potential $E_R$ for the potential plateau

The dependence of reversible potential,  $E_R$  on alkali and water activity can be fitted to an empirical equation of the form:<sup>21)</sup>

$$E_R = E_0' - p \log a_{\text{MOH}} + q \log a_{\text{H}_2\text{O}} \quad (6)$$

where  $E_0'$  is the formal potential and p and q are constants. Values of p and q were calculated from the experimental  $E_R$  values.

The overall generalized cell reaction for a Ni(OH)<sub>2</sub>/NiOOH couple against a Hg/HgO/MOH reference electrode may be written:



where U and V (in the  $\beta$ -phase system) or U' and V' (in the  $\alpha/\gamma$ -phase system) denote the coexisting phases. The quantity  $\omega$  is defined as 2/number

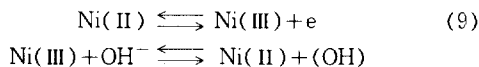
of electrons required to oxidize 1 mol of phase U (or U') to V (or V') and depends on the compositions of the pairs of coexisting phases. In the potential range where the potential is independent of the state of oxidation of the nickel, a simplified Nemst equation can be written devoid of terms for the solid phases:

$$E_R = E_0' + 2.303 \frac{RT}{2F} \log \frac{(a_{\text{H}_2\text{O}})^{1+y_1-y_2}}{(a_{\text{MOH}})^{z_2-z_1}} \quad (8).$$

The quantity  $E_0'$  is the formal potential,  $a_{\text{H}_2\text{O}}$  and  $a_{\text{MOH}}$  are the activities of H<sub>2</sub>O and alkali respectively, and RT and F have their usual significance.

### 3.4 Excess capacity of nickel hydroxide

Coulometry and analysis for active oxygen indicate an upper limit of NiO<sub>1.5</sub> for the composition of  $\beta$ -NiOOH. However, for the  $\alpha/\gamma$  couple, compositions up to NiO<sub>1.85</sub> are frequently encountered.<sup>22,23)</sup> Voltammetric data often show that the anodic to cathodic charge ratio is greater than one.<sup>22,24)</sup> Most authors ascribe these effects to the formation of Ni(IV) species.<sup>22,25)</sup> An interesting alternative proposal was made by Carbonio and co-workers.<sup>26)</sup> They studied the effects of oxygen reduction and OH<sup>-</sup> ion concentration on the  $\alpha/\gamma$  reaction. They ascribed the excess capacity to the underpotential oxidation of OH<sup>-</sup> ions that are inserted into the nickel hydroxide layers and proposed the following reaction scheme:



where the parentheses denote incorporation into the Ni(OH)<sub>2</sub>/NiOOH layer.

## 4. Transport processes in nickel hydroxide films

### 4.1 Proton diffusion in the nickel hydroxide electrode

Proton diffusion in the nickel hydroxide and nickel oxyhydroxide electrode has been studied by

\* This term is sometimes called insertion(desertion) or charging(discharging) in the literature.

many researchers with various techniques such as cyclic voltammetry,<sup>27)</sup> current transient,<sup>23,28)</sup> and optical absorption transient.<sup>27)</sup> Proton diffusion coefficient determined at room temperature ranged between  $10^{-8}$  and  $10^{-13}$   $\text{cm}^2 \text{s}^{-1}$ , depending on the crystal structure and measuring techniques.

The oxidation of the nickel hydroxide electrode is believed to proceed by a reversible one electron transfer step at the nickel ion site in the nickel hydroxide lattice. This produces a Ni(III) ion and releases a proton. The proton diffuses from the oxidation site to the electrode-electrolyte interface where it reacts with an hydroxyl ion to form a water molecule.

The cyclic voltammetric peak current  $i_p$  is directly proportional to the square root of the scan rate  $V$ , which is given by<sup>30)</sup>

$$i_p = 2.7 \times 10^5 n_e^{3/2} A D^{1/2} C_0 V^{1/2} \quad (10)$$

where  $n_e$  is the number of electrons transferred,  $A$  is the electrode area,  $D$  is the diffusion coefficient of rate determining species, i.e., proton, and  $C_0$  is the proton concentration.  $D$  can be determined from the slope of  $i_p$  vs.  $V^{1/2}$  plot.

From the potentiostatic current transient during hydrogen intercalation and deintercalation, diffusion coefficient can also be obtained. For the planar electrode, the proton diffusion is one dimensional diffusion problem. In this case, if the initial concentration of protons in the lattice is constant at the value  $C_0$  through the depth of the film and zero everywhere else. This problem is the familiar heat transfer problem and the measured current as a function of time can be expressed<sup>30)</sup>

$$i_{\text{diff}} = \frac{n_e F A D^2 C_0}{h} \sum_{n=0}^{\infty} \exp \left\{ \frac{-D \pi^2 (2n+1)^2 t}{4h^2} \right\} \quad (11)$$

where  $h$  is the film thickness,  $\pi$  has the usual meaning,  $n$  is the integer, and  $t$  is the time from the start of the diffusion process. This series, Eq. (11), which is valid for the finite boundary value problem, converges rapidly even for small times if the ratio  $D/h^2$  is sufficiently large.  $C_0$  is assumed

to be equal to the concentration of nickel sites in the nickel hydroxide lattice, since one proton is released at each nickel site, and is expressed in mole  $\text{cm}^{-3}$ .

From the current transient measurements, MacArthur<sup>28)</sup> reported that the activation energy  $\Delta E$  for the protons diffusing in oxidized and reduced materials were 9.2 and 9.6  $\text{kJ deg}^{-1} \text{mole}^{-1}$ . They suggested that the small temperature dependence of the diffusion coefficient clearly demonstrates that the protons move through the lattice by a simple diffusion process rather than by a jumping from one oxygen atom to the next.

Simple proton diffusion model in the homogeneous phase was criticized by Glarum and Marshall.<sup>30)</sup> They argued from ac-impedance study that a rapid bulk response with no indications of limitation by ion diffusion within the film is attributable to the phase boundary propagation within individual grains. More recently, Yang and Pyun<sup>31)</sup> proposed a theoretical description of the current transient for the diffusion process occurring in the two-phase coexisting material. They regarded the diffusion in the two-phase region as a problem of trapping and detrapping. They considered the diffusant rich phase as trap sites for diffusant and demonstrated that the approach can be generally applied to the intercalating systems such as Pd, LaNi<sub>5</sub>, anodic V<sub>2</sub>O<sub>5</sub> film, and amorphous WO<sub>3</sub> sputtered film.

#### 4.2 Proposal to the future work

Hydrous oxy-hydroxide films can generally be classified as space distributed redox electrode consisting of redox centers uniformly distributed in a layer of thickness  $L$ , limited on one side by the metal electrode and on the other by the aqueous solution. Nickel hydroxide prepared by chemical or electrochemical methods usually consists of very fine particles (few nanometers). The fine microstructure gives high reactivity upon intercalating and deintercalating. On the other hand, this makes it difficult to determine the active area and hence quantitative study is restricted. So, other prepara-

tion methods such as sputtering or spin-coating should be recommended for more quantitative study.

Proton diffusion through the single phase of nickel hydroxide or oxyhydroxide has rarely been studied probably because nickel hydroxide and oxyhydroxide have relatively narrow hydrogen solubility limit of about 15%. Most investigations have disregarded phase boundary movement occurring during proton intercalation or deintercalation into/from the nickel hydroxide electrode. In fact, proton intercalation/deintercalation is accompanied by phase boundary movement. The problem of proton diffusion involving phase boundary movement is not only confined to the nickel hydroxide system but also is extended to other intercalation systems. A new experimental method or new mathematical model is required to solve the problem of diffusion involving phase boundary movement.

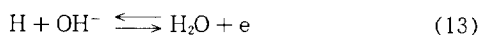
The mobility of phase boundary movement during intercalation or deintercalation can be determined by extending the new approach recently proposed by Yang and Pyun.<sup>31)</sup> Also, by extending this approach, quantitative informations about proton diffusion through a single phase such as diffusion coefficient and activation energy can be determined. Another method to determination of proton diffusion through a single phase is electrochemical hydrogen permeation. From the hydrogen permeation through a bilayer obtained by depositing nickel hydroxide onto a hydrogen permeable membrane such as Pd, one can make determination of quantitative parameters in the single phase.

Nickel hydroxide has much lower electronic conductivity than that of nickel oxy-hydroxide. The electronic conductivity depends upon the composition of the electrodes. Electric field across the electrode should be considered in the case of low electron conductivity. In addition, junction type(p/n or n/p) and direction of bias(forward or reverse) should be taken into consideration.

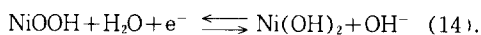
## 5. Self-discharge of the nickel hydroxide electrode

There are at least three possible mechanisms for the self-discharge reaction in an Ni/H<sub>2</sub> cell: (i) hydrogen reduces nickel oxyhydroxide(NiOOH) via a chemical reaction; (ii) hydrogen adsorbs on the nickel substrate on one site, at which an electrochemical oxidation occurs, while NiOOH is reduced to Ni(OH)<sub>2</sub> at another nearby site in the counterelectrode reaction; or (iii) NiOOH reacts with water to give Ni(OH)<sub>2</sub> and oxygen gas, which in turn reacts with hydrogen to form water.

If the kinetics and/or mechanism of NiOOH reduction involve electrochemical reactions, then the oxidation process for hydrogen will be<sup>32)</sup>



with simultaneous reduction of  $\beta$ -NiOOH to  $\beta$ -Ni(OH)<sub>2</sub>



If a direct chemical reaction occurs between hydrogen and nickel oxide, the reduction reaction will be

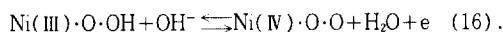


Assuming the overall self-discharge process is given by reaction (15) and using available thermodynamic data, the total amount of heat that will be involved during complete discharge, which should be proportional to the enthalpy change of the reaction (15), was estimated to be -144.85 kJ/mol or -5.404kJ/Ah at 25°C.

Conway and Bourgault<sup>33)</sup> showed that the oxygen evolution reaction can be the rate determining step in the self-discharge of the nickel electrode. On thin films anodically formed on Ni surfaces, there are two Tafel regions for oxygen evolution,

one with a slope of 39-44 mV dec<sup>-1</sup> at lower current density.

In the potential region of about 0.6V, the slope smoothly changes to 58-65 mV dec<sup>-1</sup>.<sup>33)</sup> The low Tafel slope region is coupled with an appreciable pseudo capacitance of the intermediates. This implies that an electrochemical desorption step is rate controlling with the coverage by intermediates dependent on the potential. The higher Tafel slope implies a one-electron quasi-equilibrium prior to a chemical rate-controlling step of the first order. The proposed intermediates in the low-current density region are Ni(IV) sites on the nickel oxide surface with relatively low coverage. The state of the surface is determined by the reaction



The proposed chemical step in the high current density region is



## 6. Electrochromism in nickel hydroxide electrode

### 6.1. H intercalation reaction in nickel hydroxide electrode

The electrochemical oxidation reaction is generally written as

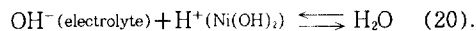


However, electrochemical reactions takes place at the boundary where there is a transition between ionic conduction and electronic conduction. Since Ni(OH)<sub>2</sub> is predominantly an ionic conductor (a solid electrolyte) the electrochemical reaction occurs at the Ni(OH)<sub>2</sub>/NiOOH interface, where neither H<sub>2</sub>O nor OH<sup>-</sup> are present. The electrochemical reaction should therefore more properly be written as



It has long been known<sup>34)</sup> that the NiOOH forms first at the interface between the Ni(OH)<sub>2</sub> and the underlying electronic conductor, rather than at the electrolyte/Ni(OH)<sub>2</sub> interface. Other authors<sup>21, 35)</sup> have observed the motion of the color boundary during charge/discharge of such electrodes.

In order for the oxidation reaction to proceed, the protons must be transported away from the interface through the galleries in the Ni(OH)<sub>2</sub> phase and into the electrolyte. However, in the alkaline aqueous electrolyte environment hydrogen is not present as either H<sup>+</sup> or H<sub>2</sub>. Instead, hydrogen is transferred between the electrolyte and the Ni(OH)<sub>2</sub> phase by the interaction of neutral H<sub>2</sub>O molecules and OH<sup>-</sup> ions in the electrolyte with the H<sup>+</sup> ions at the electrolyte/Ni(OH)<sub>2</sub> interface. Thus the reaction at the electrolyte/Ni(OH)<sub>2</sub> interface must be electrically neutral and can be written as



In earlier works on sputtered NiO<sub>x</sub> films the hypothesis was made that electrochemical pretreatment of NiO<sub>x</sub> electrodes was necessary in order to hydrate the film to activate its electrochromic behaviour.<sup>36,37)</sup> The experiments with the palladium overlayer on the sputtered NiO<sub>x</sub> films<sup>38)</sup> showed that it is not necessary to make the contact with water to perform coloring-bleaching cycles with sputtered NiO<sub>x</sub> film. This is in accordance with the results found by IR spectroscopy,<sup>39)</sup> that did not show any evidence for water incorporation into the NiO<sub>x</sub> film, even after extensive electrochemical cycling.

The as-deposited sputtered films are considered to be a mixture of two phases, NiO and Ni<sub>3</sub>O<sub>4</sub>.<sup>36)</sup> In this case, the bleaching/coloring reactions for sputtered films should be formally written as



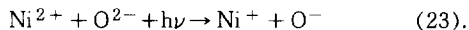
or by means of its electrochemical equivalent.



From the results of electrochemical quartz microbalance study,<sup>38)</sup> the linear relationship between stress and charge is observed more evidently during ion intercalation than during ion deintercalation. This could be related to the faster kinetics observed previously for the bleaching reaction. The compressive tension value reported above is comparable with the experimental values observed for H intercalation in Metallic Pd films<sup>40)</sup> and for Li<sup>+</sup> intercalation in NiO, film (13 MPa/mC cm<sup>-2</sup> μm<sup>-1</sup> and 8 MPa/mC cm<sup>-2</sup> μm<sup>-1</sup>, respectively).<sup>5)</sup>

## 6.2 Nature of electrochromic reaction

There is considerable disagreement as to the exact nature of the electronic excitation which gives rise to anodic electrochromism. Some authors<sup>41,42)</sup> state that the principal absorbance in the visible-near u.v. region are charge transfer related



Alternatively more recent interpretations which take into account electronic correlation and electron-phonon coupling describe the excitation

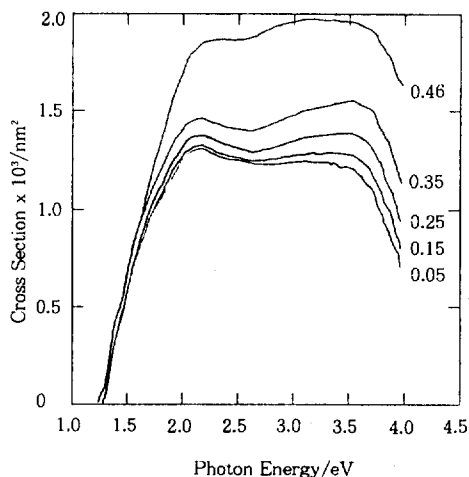


Fig. 4. Optical absorption cross section of an electrochromic NiO film at the indicated potentials in  $V_{\text{scan}}$ . The bleached state transmittance was measured at  $-0.15 V_{\text{scan}}$  and the electrolyte was 0.01 M KOH.<sup>44)</sup>

as allowed transitions of the ground-state metal ions.

For a central Ni<sup>2+</sup> ion surrounded by six O<sup>2-</sup> ions, the optical behaviour is similar to that of stoichiometric NiO or Ni(OH)<sub>2</sub>. The minimum energy for strong absorption is about 4eV, and corresponds to the "bandgap" transition 3d<sup>8</sup> → 3d<sup>9</sup>L, where L denotes a hole on an O<sup>2-</sup> ligand (that is, an O<sup>-</sup> ion).<sup>43)</sup>

If the Ni(OH)<sub>2</sub> cluster is "oxidized" so that it now consists of a central Ni<sup>2+</sup> ion surrounded by five O<sup>2-</sup> ions and one O<sup>-</sup> ion, two new absorption bands are expected, and these may account for the bands seen in Fig. 4.<sup>44)</sup> Transfer of the hole from one oxide ion to another results in optical absorption because the electronic transition is strongly coupled to the vibrational modes of the cluster. By analogy to O<sup>-</sup> centers in MgO and CaO, the oxide to oxide transfer is expected to produce a broad absorption band centered at about 2 eV, which can be described in a configuration coordinate scheme.<sup>45)</sup> The other new absorption band is associated with the transition 3d<sup>8</sup>L → 3d<sup>7</sup>, which is expected to have an energy close to the "bandgap" value, and this may account for the 3.4 – 3.5 eV band in Fig. 4.

## 7. Effect of foreign ions

### 7.1 Lithium

The major effect of lithium addition is an increase in the oxygen overvoltage and the elimination of the poisoning effects of iron.<sup>46,47)</sup> Large amounts of Li<sup>+</sup> ions are incorporated into the lattice during oxidation of  $\alpha$ -Ni(OH)<sub>2</sub> in LiOH. Strongly absorbed Li<sup>+</sup> is also found in  $\beta$ -Ni(OH)<sub>2</sub> electrodes that are charged in LiOH electrolytes.

### 7.2 Iron

Significant decreases were observed in the oxygen overvoltage with as little as 0.01% coprecipitated iron. Iron contents of 1% and above significantly decreased the electrode capacity.

### 7.3 Cobalt

Cobalt is added to nickel oxide electrodes to improve the charge efficiency, particularly at higher temperatures. It also has other beneficial effects in that it mitigates electrode swelling,<sup>48,49)</sup> minimizes the number of formation cycles,<sup>50)</sup> and eliminates the second plateau discharge in plasticbonded nickel oxide electrodes.<sup>51)</sup> One effect of cobalt is to inhibit the formation of  $\gamma$ -NiOOH on charge. The most important effect may be to decrease the working potential of the electrode slightly and to increase the reversibility of the Ni(II)/Ni(III) reaction. Recent XANES results indicate that cobalt maximizes the degree of oxidation of the nickel.

### 7.4 Cadmium

Addition of Cd<sup>+</sup> inhibits electrode swelling and formation of  $\gamma$ -NiOOH.<sup>52)</sup> The cadmium addition appears to have purely a surface effect.

### 7.5 Zinc

It has a poisoning effect that is a pore plugging effect and not a chemical effect on the nickel oxide electrode.<sup>49)</sup> In the absence of plugging, the addition of zincate is beneficial. It inhibits the formation of  $\gamma$ -NiOOH, reduces electrode swelling and increases the oxygen overvoltage.

## 8. Conclusions and future work

In the present review article, we have summarized the works on the nickel hydroxide electrode previously published in the literature involving structural and textural characteristics, electrochemical processes, transport processes, self discharge, electrochromism, and additive effects from the electrochemical view points. Also, several basic ideas chiefly on the proton diffusion were suggested for the future work.

Much of the electrode behaviour depends upon the solid state properties. Thus, solid state properties involving composition, microstructure, and semiconducting properties of the various nickel

oxide phases should be quantified.

Kinetics of ion intercalation and deintercalation into/from an electrode significantly depends on the surface character of the electrode. In many cases nickel hydroxide, when in contact with aqueous media, contain considerable quantities of loosely bound and trapped water, and electrolyte species. So, the relationship between surface chemistry of the electrode and surface reactions involving absorption and deintercalation of ions needs to be clarified.

The most important and least understood areas of the electrode kinetics are proton diffusion in the presence of phase boundary movement and effect of electric field on proton diffusion. Therefore, the relationship between proton diffusion and composition, and structure of the electrode should be elucidated, considering the phase boundary movement and electric field across the electrode.

The self-discharge mechanism of hydrogen/nickel hydroxide batteries requires further work. The respective contributions of the current collector and active material should be identified.

## References

1. L. D. Burke and M. E. G. Lyons, "Modern Aspects of Electrochemistry", Vol. **18**, Chap. 4, Ed. by R. E. White, J. O'M. Bockris, and B. E. Conway, Plenum Press, New York, p. 169 (1990).
2. H. E. G. Rommal and P. J. Moran, *J. Electrochem. Soc.*, **132**, 325(1985).
3. M. Amjad, D. Pletcher, and C. Smith, *J. Electrochem. Soc.*, **124**, 203(1977).
4. J. Scarminio, W. Estrada, A. Andersson, A. Gorenstein, and F. Decker, *J. Electrochem. Soc.*, **139**, 1236(1992).
5. I. C. Faria, R. Torresi, and A. Gorenstein, *Electrochim. Acta*, **38**, 2765(1993).
6. J. McBreen, "Modern Aspects of Electrochemistry", Vol. **21**, Chap. 2, Ed. by R. E. White, J. O'M. Bockris, and B. E. Conway, Plenum Press, New York, p.29(1990)

7. H. Bode, K. Dehmelt, and J. Witte, *Electrochim. Acta*, **11**, 1079(1966).
8. M. Oshitani, T. Takayama, K. Takashima, and S. Tshuji, *J. Appl. Electrochem.*, **16**, 403 (1986).
9. R. S. McEwen, *J. Phys. Chem.*, **75**, 1782 (1971).
10. S. Le Bihan and M. Figlarz, *J. Cryst. Growth*, **13/14**, 458(1972).
11. F. P. Kober, *J. Electrochem. Soc.*, **112**, 1064 (1965).
12. F. P. Kober, *J. Electrochem. Soc.*, **114**, 215 (1967).
13. R. S. Schrebler Guzman, J. R. Vilche, and A. J. Arvia, *J. Appl. Electrochem.*, **9**, 321(1979).
14. R. Barnard, G. T. Crickmore, J. A. Lee, and F. L. Tye, *J. Appl. Electrochem.*, **10**, 61(1980).
15. R. S. Schrebler Guzman, J. R. Vilche, and A. J. Arvia, *J. Electrochem. Soc.*, **125**, 1578 (1978).
16. J. P. Hoare, "The Electrochemistry of Oxygen", John Wiley & Sons, New York(1968).
17. L. D. Burke and T. A. M. Twomey, *J. Electroanal. Chem.*, **134**, 353(1982).
18. R. Barnard, C. F. Randell, and F. L. Tye, *J. Appl. Electrochem.*, **11**, 517(1981).
19. F. Portemer, A. Delahaye-Vidal, and M. Figlarz, *J. Electrochem. Soc.*, **139**, 671(1992).
20. I. C. Faria, R. Torresi, and A. Gorenstein, *Electrochim. Acta*, **38**, 2765(1993).
21. R. Barnard, C. F. Randell, and F. L. Tye, *J. Appl. Electrochem.*, **10**, 109(1980).
22. D. A. Corrigan and P. R. Snodin, *Electrochim. Soc.*, **136**, 613(1989).
23. G. W. D. Briggs and P. R. Snodin, *Electrochim. Acta*, **27**, 565(1982).
24. R. Barnard, C. F. Randell, and F. L. Tye, "Power Sources 8", Ed. by J. Thompson, Academic press, London, p.401(1981).
25. J. Desilvestro, D. A. Corrigan, and M. G. Weaver, *J. Electrochem. Soc.*, **135**, 885(1988).
26. R. E. Carbonio, V. A. Macagno, and A. J. Arvia, *J. Electroanal. Chem.*, **177**, 217(1984).
27. C. Zhang and S-M. Park, *J. Electrochem. Soc.*, **134**, 2966(1987).
28. D. M. MacArthur, *J. Electrochem. Soc.*, **117**, 729(1970).
29. A. J. Bard and L. R. Faulkner, "Electrochemical Methods", Chap. 6, John Wiley & Sons, New York,(1986).
30. S. H. Glarum and J. H. Marshall, *J. Electrochem. Soc.*, **129**, 535(1982).
31. T.-H. Yang and S.-I. Pyun, in preparation for publication(1995).
32. Y. J. Kim, A. Visintin, S. Srinivasan, and A. J. Appleby, *J. Electrochem. Soc.*, **139**, 351 (1992).
33. B. E. Conway and P. L. Bourgal, *Can. J. Chem.*, **40**, 1690(1962).
34. R. A. Huggins, H. Prinz, M. Wohifahrt-Mehrens, L. Jorissen, and W. Witschel, *Solid State Ionics*, **70/71**, 417(1994).
35. G. W. D. Broggs amd M. Fleischmann, *Trans. Faraday Soc.*, **67**, 2397(1971).
36. J. S. E. M. Svensson and C. G. Granqvist, *Solar Ener. Mater.*, **16**, 19(1987).
37. W. Estrada, A. Andersson, and C. G. Granqvist, *J. Appl. Phys.*, **64**, 3678(1988).
38. J. Scarminio, W. Estrada, A. Andersson, A. Gorenstein, and F. Decker, *J. Electrochem. Soc.*, **139**, 1236(1992).
39. W. Estrada, A. Andersson, C. G. Granqvist, A. Gorenstein, and F. Decker, *J. Mater. Res.*, **6**, 1715(1991).
40. J. Scrmínio, S. N. Sahu, and F. Decker, *J. Phys. E*, **22**, 755(1989).
41. K. A. Wickersheim and R. A. Lefever, *J. Chem. Phys.*, **36**, 844(1962).
42. R. Newman and R. M. Chrenko, *Phys. Rev.*, **114**, 1507(1959).
43. A. Fujimori and F. minami, *Phys. Rev. B*, **30**, 957(1984).
44. D. A. Wruck and M. Rubin, *J. Electrochem. Soc.*, **140**, 1097(1993).
45. O. F. Schirmer, K. W. Blazey, W. Berlinger, and R. Diehl, *Phys. Rev. B*, **11**, 4201(1975).
46. R. D. Armstrong, A. K. Sood, and M. Moore, *J. Appl. Electrochem.*, **15**, 603(1985).

47. R. D. Armstrong, G. W. D. Briggs, and M. Moore, *Electrochim. Acta*, **31**, 25(1986).
48. M. E. Folger, J. R. Vilche, and A. J. Arvia, *J. Electroanal. Chem.*, **172**, 235(1984).
49. R. D. Armstrong, G. W. D. Briggs, and E. A. Charles, *J. Appl. Electrochem.*, **18**, 215(1988).
50. W. Lee, *J. Electrochem. Soc.*, **132**, 2835 (1985).
51. B. Klapste, J. Mrha, K. Micak, J. Jindra, and V. Maracek, *J. Power Sources*, **4**, 349(1979).
52. P. Olivia, J. Leonardi, J. F. Laurent, C. Delmas, J. J. Bracconier, M. Figlarz, F. Fievet, and A. de Guibert, *J. Power Sources*, **8**, 229 (1982).